Model for a Fluid-Particle Breakup in a Turbulent Flow.

Zedníková, Mária
2017

DOI: https://doi.org/10.14311/TPFM.2017.042

MODEL FOR A FLUID-PARTICLE BREAKUP IN A TURBULENT FLOW

M. Zedníková[1], J. Vejražka[1], P. Stanovský

[1] **Institute of Chemical Process Fundamentals, Rozvojová 2/135, CZ-165 02 Prague 6, Czech Republic**

Abstract

A model is developed for predicting the outcome of breakup of a fluid particle (bubble or drop), which is initially deformed (e.g. due to turbulence) and breaks into two daughter particles. An initially dumbbell-shaped deformation of the particle is assumed. The evolution of sizes of particle sub-parts is calculated using Rayleigh-Plesset equations, which consider the inertia of surrounding fluid, capillary action and viscous effects. The redistribution of internal fluid in the particle is calculated using Bernoulli equation. The model computes the sizes of daughter particles after the breakup. By assuming various initial conditions (various initial shapes and initial velocities of deformation), the size distribution of daughter particles is obtained. These size distributions are qualitatively compared with available experimental data and reasonable agreement is observed. Because of strong assumptions, this model cannot be used directly for accurate prediction of size distribution after a breakup. However, it provides an insight in the physics of the breakup, especially on the effect of inner phase properties.

Keywords: bubble breakup, drop breakup, turbulent flow, breakup model

1 Introduction

The multiphase gas-liquid and liquid-liquid systems are widely used in many industrial applications (e.g. oil-water processing, boilers, bubble columns, stirred tank reactors, ejectors, air-lift reactors, etc.). Breakup of dispersed particles (bubbles or drops) is one of the processes controlling the behaviour of these multiphase systems and also the mass transfer between the phases.

As the detailed description of multiphase turbulent flows is quite complex, the computational methods help to predict the dynamic behaviour. In the case of multiphase mixtures, the Population-Balance Modelling is an increasingly popular approach. This method requires an information about the probability of breakup of particles and about the size distribution of daughters generated by the breakup; models predicting these features are reviewed in [1-3]. Most of these models predict the breakup frequency and size distribution of daughters in dependence on the local rate of energy dissipation and particle size, but surprisingly do not consider the flow of internal phase. In contrast, experiments suggest that the particle breakup in turbulent flow significantly depends on the properties of the internal phase [4], and similar behaviour has been observed also in our experimental investigation [5, 6].

A recent breakup model of Xing et al. [7] tried to explain the size distribution of daughter particles. This model assumes the initial shape of particle in form of a dumbbell and uses Young-Laplace and Bernoulli equations to describe the flow of inner phase in the particle (bubble/drop) and its redistribution among the two emerging daughters. Their model is however somewhat dubious because the inertia of outer phase is neglected. A more detailed analysis reveals that this approach can be justified only in the case of bubbles or drops with very small neck, which seems to be irrelevant for real breakup.

The aim of this paper is therefore to develop an equivalent of Xing's et al. model, which correctly computes the stresses due to inertia of surrounding liquid. This leads to a model, which considers initially deformed bubble or drop. Assuming that the shape of particle evolves as a result of inertial, capillary and viscous forces, the model estimates the outcome of binary breakup, especially the daughter sizes. This model is then used to simulate the outcome of many breakups with different initial conditions. Size distribution of daughters for breakup triggered by random events is thus obtained and it is compared with our previous experimental findings [6].

2 Model development

The concept of the model is adopted from that of Xing at al. [7]. The dumbbell shape of the breaking particle is assumed (Fig. 1). It consists of three parts: larger spherical particle with radius R_1, smaller

spherical particle with radius R_2 and a cylindrical neck with radius R_N and length L_N. The evolution of size of each part is described by Rayleigh-Plesset equations [8], which includes the inertia, capillary and viscous effects of the external phase. Similarly, the evolution of neck diameter is described by a cylindrical variant of Rayleigh-Plesset equation [9]. These three parts of the particle are hence described by a system of three ordinary differential equations for radii R_1 and R_2 of spherical parts and neck radius R_N:

$$\ddot{R}_1 = -\frac{3}{2}\frac{\dot{R}_1^2}{R_1} + \frac{P_1 - P_\infty}{\rho R_1} - \frac{2\sigma}{\rho R_1^2} - \frac{4\mu\dot{R}_1}{\rho R_1^2} \tag{1}$$

$$\ddot{R}_2 = -\frac{3}{2}\frac{\dot{R}_2^2}{R_2} + \frac{P_2 - P_\infty}{\rho R_2} - \frac{2\sigma}{\rho R_2^2} - \frac{4\mu\dot{R}_2}{\rho R_2^2} \tag{2}$$

$$\ddot{R}_N = -\frac{\dot{R}_N^2}{R_N}\left(1 - \frac{1}{2ln\frac{R_\infty}{R_N}}\right) + \frac{P_N - P_\infty}{\rho R_N ln\frac{R_\infty}{R_N}} - \frac{\sigma}{\rho R_N^2 ln\frac{R_\infty}{R_N}} - \frac{2\mu\dot{R}_N^2}{\rho R_N^2 ln\frac{R_\infty}{R_N}} \tag{3}$$

here $\dot{R}$ and $\ddot{R}$ are the first and second time derivative of the radii, respectively. The derivatives of the radii in equations (1-3) need to match the volume-conservation constraint

$$V_{tot} = \text{const} = 4/3\pi R_1^3 + 4/3\pi R_2^3 + \pi R_N^2 L_N \tag{4}$$

here L_N is the length of the neck. After differentiating this equation, we get the constraint for first derivatives $[\dot{R}_1, \dot{R}_2, \dot{R}_N]$

$$0 = 2R_1^2\dot{R}_1 + 2R_2^2\dot{R}_2 + L_N R_N \dot{R}_N \tag{5}$$

Another differentiating gives a constraint for second derivatives $[\ddot{R}_1, \ddot{R}_2, \ddot{R}_N]$

$$0 = 2R_1^2\ddot{R}_1 + 2R_2^2\ddot{R}_2 + L_N R_N \ddot{R}_N + 4R_1\dot{R}_1^2 + 4R_2\dot{R}_2^2 + L_N\dot{R}_N^2 \tag{6}$$

Note that equation (6) cannot guarantee volume conservation because any linear time evolution of total volume $V_{tot} = c_1 + c_2 t$ satisfies the equation (6). However, it can still be used as a constraint for second derivatives $[\ddot{R}_1, \ddot{R}_2, \ddot{R}_N]$ as long as the first derivative of volume conservation (5) is satisfied.

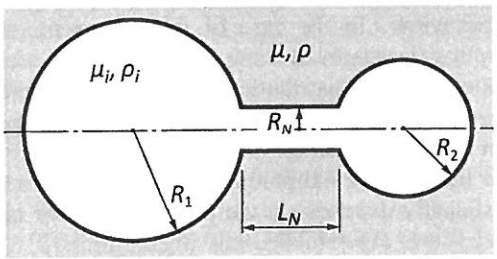

Figure 1: Dumbbell shape of the breaking fluid particle

The system of differential equations (1-3) with the constraints (5,6) contains additional unknowns $[P_1, P_2, P_N]$ and parameters $[L_N, R_\infty, P_\infty, \rho, \mu, \sigma]$, which are estimated from additional assumptions of the model:

1. The overall particle size before breakup is D = 5mm (matching typical size of our experiments [6]).
2. Only binary breakups are assumed.
3. The initial volume of the neck is assumed to be 5% of the volume of the mother particle.
4. The length of the neck is kept unchanged, $L_N = D/4$.
5. The cut-off distance of neck far field is assumed $R_\infty = D$.
6. The part R_1 is always bigger than the part R_2 resulting to the pressures in the particles $P_1 < P_2$ and flow direction from the smaller particle to the bigger one; $\dot{R}_1 > 0$ and $\dot{R}_2 < 0$.
7. The pressure far enough from the particle is set to zero, $P_\infty = 0$. As we don't assume any phase changes, the system does not depend on the absolute pressure and the parameter P_∞ can be omitted.
8. Pressure loss in the neck ΔP is calculated from the Bernoulli equation; the viscous pressure drop due flow through the neck is estimated using the Hagen–Poiseuille equation. This leads to the relation between the velocity in the neck U_N and the pressure loss in form

$$\Delta P = P_2 - P_1 = \frac{1}{2}\rho_i U_N |U_N| + \frac{8\mu_i U_N L_N}{R_N^2} \tag{7}$$

9. Pressure driving the neck contraction P_N is assumed

$$P_N = \min(P_1, P_2) + \frac{4\mu_i U_N L_N}{R_N^2} \tag{8}$$

10. Velocity in the neck U_N used in equations (7-8) is determined from the conservation; increase of the radius R_1 is caused by the fluid flow through the neck

$$4\pi R_1^2 \dot{R}_1 = -\pi R_N^2 U_N \quad => \quad U_N = -\frac{4R_1^2 \dot{R}_1}{R_N^2} \tag{9}$$

11. To compare the model results with available experimental data [6], water is assumed as the outer phase and air bubbles and cyclohexane drops, respectively, as the inner phase. The physical-chemical properties of used fluids are listed in Table 1.

Table 1: Physical-chemical properties of assumed fluids

Fluid property	Water	Air	Cyclohexane
density, ρ [g/cm^3]	0.998	0.001	0.779
viscosity, μ [mPa.s]	1.00	0.02	1.02
surface tension, σ [mN/m]	70.9	-	25.0
interfacial tension (with water), σ [mN/m]	-	70.9	49.0

2.1 Calculation procedure

The system described above is a system of ordinary differential equations (1-3) with unknowns [R_1, $\dot{R}_1$, R_2, $\dot{R}_2$, R_N, $\dot{R}_N$] (defining the state vector), the constraints (5,6) and algebraic equations (7-9) with additional unknowns [P_1, P_2, P_N, U_N]. Equations contain also [L_N, R_∞, P_∞, ρ, μ, σ], which are parameters of the system. The initial conditions are chosen to get various initial volume distribution between the parts R_1 and R_2 and various growing rates of the particles $\dot{R}_1$, $\dot{R}_2$ (Table 2). The initial condition for the shrinking of the neck $\dot{R}_{N0}$ comes from the total volume conservation after taking the first derivative (5).

Table 2: Initial conditions for differential equations (1-3)

Initial neck radius is calculated with respect to assumptions 3 and 4.	$R_{N0} = 0.92$ mm
Initial radius of larger particle ranges in interval	$R_{10} \in \langle 2.36 - 1.97$ mm$\rangle$
Initial radius of smaller particle is calculated from R_{N0} and R_{10} assuming the total volume conservation	$R_{20} \in \langle 1.18 - 1.93$ mm$\rangle$
Initial first derivative $\dot{R}_{10}$ ranges in interval	$\dot{R}_{10} \in \langle 0 - 0.3$ m/s$\rangle$
Initial first derivative $\dot{R}_{20}$ ranges in interval	$\dot{R}_{20} = -\dot{R}_{10}$
Initial first derivative $\dot{R}_{N0}$ is calculated from the equation (5)	$\dot{R}_{N0} = -2R_{10}^2/(L_N R_N)\dot{R}_{10} - 2R_{20}^2/(L_N R_N)\dot{R}_{20}$

When solving a time step, the state vector [R_1, $\dot{R}_1$, R_2, $\dot{R}_2$, R_N, $\dot{R}_N$] is known (from either previous time step or initial condition). The second derivatives [$\ddot{R}_1, \ddot{R}_2, \ddot{R}_N$] together with unknowns [P_1, P_2, P_N, U_N] have to be solved. As the system of equations (1-3, 7-9) is implicit for one variable, an iterative procedure has to be used. The calculation procedure is as follows:

1. The pressure P_1 is guessed.
2. U_N, P_2 and P_N are computed from equations (7-9).
3. Second derivatives [$\ddot{R}_1, \ddot{R}_2, \ddot{R}_N$] are computed from differential equations (1-3).
4. Right-hand side of equation (6) is evaluated.
5. The pressure P_1 is then adjusted (and U_N, P_2, P_N, $\ddot{R}_1, \ddot{R}_2$ and $\ddot{R}_N$ are recalculated correspondingly) in the way that equation (6) is satisfied. For iterating appropriate value of P_1, regula falsi method (with cubic spline interpolation) is used until uncertainty of P_1 is smaller than $10^{-5}\sigma/D$.
6. After finding P_1, the derivative of state vector [$\dot{R}_1, \ddot{R}_1, \dot{R}_2, \ddot{R}_2, \dot{R}_N, \ddot{R}_N$] is known and it is passed to the solver of differential equations. The solver then computes next time step (returns to point 1).

The calculations are made in software Matlab R2016a using the solver 'ode15s', which is a variable-order solver (orders 1-5) suitable for stiff problems. The calculation stops when: i. the neck radius reaches

the radius of the smaller particle $R_N = R_2$, or ii. the neck is closed (practically, we set a threshold $R_{N,stop} = 10^{-5}$ m). In the former case, the evolution of particle deformation is regarded as no breakup. In the latter case, final radii R_1 and R_2 are regarded as sizes of daughter particles after the breakup.

The validity of equations (4) and (5) is verified. There is a minor variation of total volume due to numerical accuracy, but this variation is of order of $10^{-5}V_{tot}$ (after many time steps), which is consistent with the requested accuracy on P_1. We expect the same order of residual errors also for the other differential equations. Usage of more accurate solvers (e.g 'ode45') increases the accuracy of computations by several orders of magnitude.

3 Results and discussion

The outcome from each calculation is the time evolution of radii [R_1, R_2, R_N], pressures [P_1, P_2, P_N] and velocity in the neck U_N. This evolution could finish either by particle breakup into two daughter particles (for typical example, see Fig. 2) or by diminishing of the smaller particle until it empties without breakup (Fig. 3). The difference between these two cases is in the initial particle deformation; both initial velocities for the shown examples are $\dot{R}_{10} = \dot{R}_{20} = 0$.

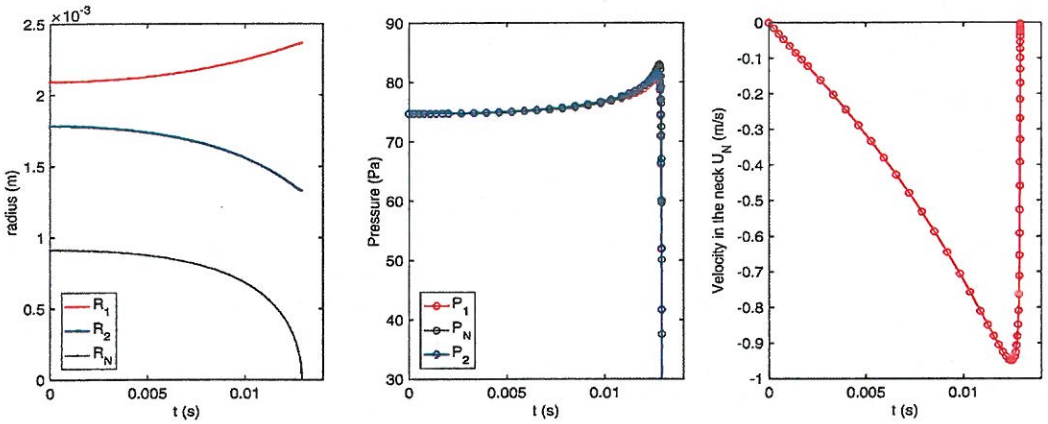

Figure 2: Evolution of radii and pressures in individual parts of the particle and evolution of the velocity in the neck resulting to the breakup. Bubble-water system, initial conditions $R_{10} = 2.09$ mm, $R_{20} = 1.78$ mm, $\dot{R}_{10} = \dot{R}_{20} = 0$, final sizes after the breakup $R_1 = 2.36$ mm, $R_2 = 1.34$ mm

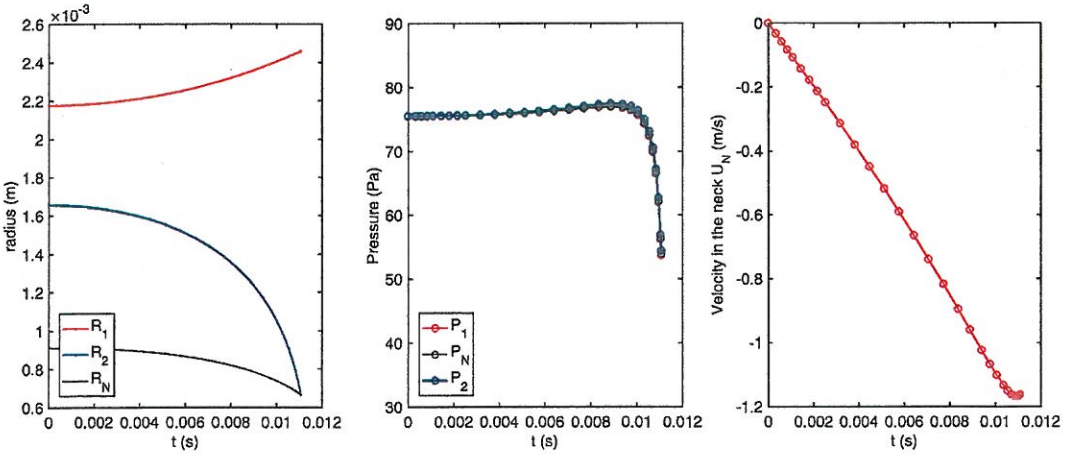

Figure 3: Evolution of radii and pressures in individual parts of the particle and evolution of the velocity in the neck resulting to the diminishing of the smaller spherical part (no breakup). Bubble-water system, initial conditions $R_{10} = 2.17$ mm, $R_{20} = 1.66$ mm, $\dot{R}_{10} = \dot{R}_{20} = 0$,

The capillarity causes the flow of internal phase from the smaller part R_2 to the bigger one because of higher capillary pressure. The velocity in the neck increases (negative sign of U_N means the flow from right side to the left one) and R_N, R_2 decreases. The effect of capillarity is counteracted by the inertia of

surrounding liquid and by the pressure drop in the neck. When the pressure drop in the neck starts to dominate over surrounding inertia, the velocity in the neck decreases until the neck either closes (breakup, Fig. 2) or merges with the part R_2 (no breakup, Fig. 3). As the pressures $[P_1, P_2, P_N]$ are function of the velocity in the neck, the drop of the pressures at the end of time evolution is also related to the prevailing effects and to the decrease of the velocity in the neck. Both cases displayed in Figures 2 and 3 were observed also experimentally [6], where the strong particle deformation could result either in the breakup or non-breakup.

The goal, for which the present model is developed, is to obtain the size distribution of daughter particles. It is assumed that in a turbulent flow, the bubble or drop is perturbed by random events. Therefore, various initial conditions (Table 2) are used and the evolution of bubble shape is calculated. By summarizing the outcome for all initial conditions, the size distribution of daughter particles is obtained (Figure 4). It is expressed in terms of the probability-density function (p.d.f.) of occurrence of daughter with given volume fraction of the mother.

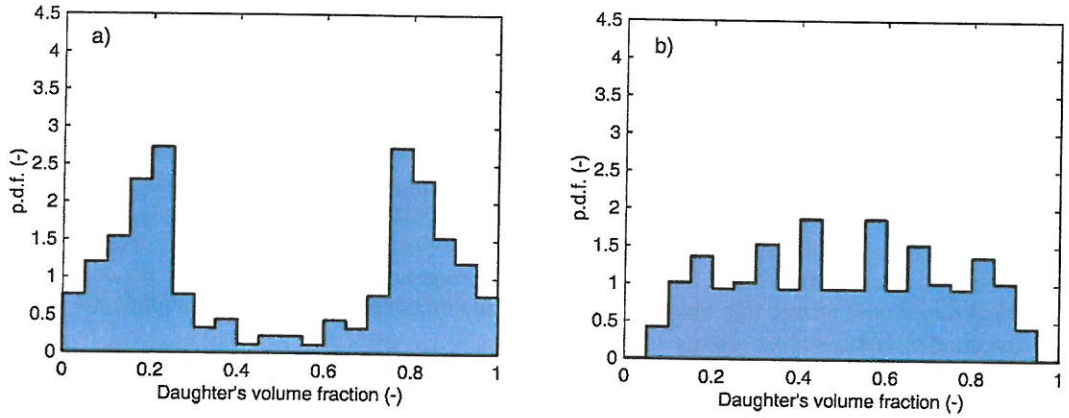

Figure 4: Computed size distribution of daughter particles: a) air bubbles in water (95 breakups, 190 data leading to p.d.f.), b) cyclohexane drops in water (118 breakups, 236 data leading to p.d.f.)

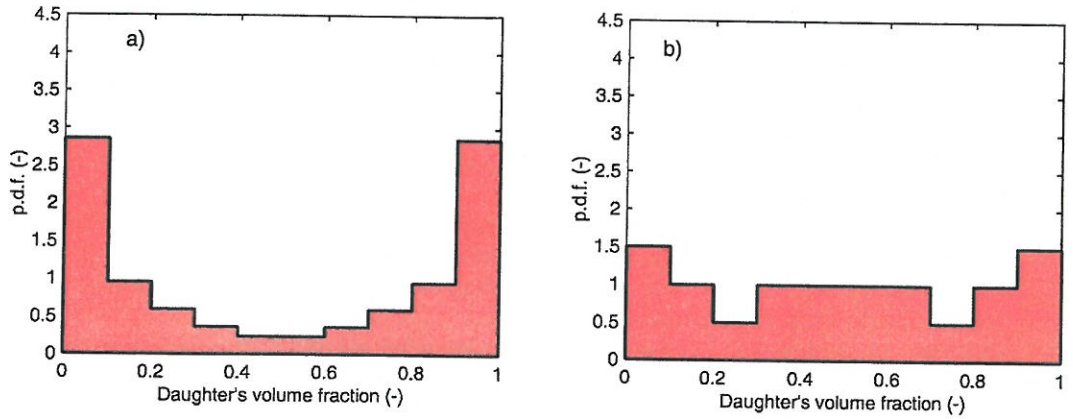

Figure 5: Experimental size distribution of daughter particles [6]. Data for binary breakups of particles with size in range $D \in \langle 4.5 - 5.5 \text{ mm} \rangle$: a) air bubbles in water (52 valid breakups), b) cyclohexane drops in water (30 valid breakups)

Even though the used range of initial conditions is quite restrictive and the amount of data leading to p.d.f. is limited, a strong qualitative difference is observed comparing the daughter size distributions for bubble and drop breakup (Figures 4a, 4b). The air bubbles with low density and viscosity of the inner phase mostly break into one large and one small bubble (the two characteristic peaks in Fig. 4a). On the other hand, the daughter size distribution for drop breakup is more uniform, leading more frequently to two daughters with comparable size. This is linked to the redistribution of the inner phase during the breakup: in the case of bubbles, the gas moves easily from one part to another, and two daughters of

uneven size are produced. Oppositely in the case of liquid drop, the flow of inner fluid through the neck is opposed by higher resistance due to high density and viscosity. Less fluid is hence redistributed between drop parts before the neck is closed.

Similar bubble and drop size distributions were obtained also experimentally [6] (Figures 5a, 5b). This suggests that the inertia and viscous effects of both inner and outer phases are important during the breakup and needs to be taken into account in its modelling. The redistribution of the internal phase in the particle seems to be a crucial for the size distribution of the daughter particles. Note that this dependence is ignored in most models for daughter size distribution (e.g. in the most frequently used model of Luo and Svendsen, [10]).

Conclusions

A model simulating the binary breakup of the fluid particle due to its initial deformation (e.g. by a turbulent flow) has been developed. It assumes the inertial, viscous and capillary effects in both inner and outer phases. The outcome of the model is the size distribution of daughter particles triggered by random events, which lead to various initial deformations of the particle and the various initial speeds of deformation. Comparing the breakup of bubbles and droplets, a significant qualitative difference in daughter size distribution is obtained. This points out that the properties of inner phase need to be taken onto account when modelling the breakup.

Note that the present model is a strong oversimplification of reality. For example, majority of breakup is not binary (as considered here) but leads to multiple daughters; initial shapes are more complicated than the assumed dumbbell shape; particles have more degrees of freedom than only three considered here; initial conditions (shape and deformation speed) were just uniformly distributed over some interval, without further justification of this interval by some real experimental statistics. Still, we believe that this oversimplified model proves that the redistribution of the inner fluid is an important phenomenon, which controls the size distribution of daughter particles.

To our knowledge, the redistribution and properties of inner fluid is disregarded in most models for daughter size distribution. We believe that any physically correct model for size distribution of daughters should take this phenomenon into account.

Acknowledgement: This research has been supported by Czech Science Foundation (project 15-15467S).

References

[1] Liao Y. & D. Lucas: A literature review of theoretical models for drop and bubble breakup in turbulent dispersions. *Chemical Engineering Science*, vol. 64, no. 15: (2009), pp. 3389-3406.

[2] Solsvik J. & H. A. Jakobsen: On the solution of the population balance equation for bubbly flows using the high-order least squares method: implementation issues. *Reviews in Chemical Engineering*, vol. 29, no. 2: (2013) pp. 63-98.

[3] Solsvik J., S. Tangen, and H. A. Jakobsen: On the constitutive equations for fluid particle breakage *Reviews in Chemical Engineering*, vol. 29, no. 5: (2013) pp. 241-356.

[4] Andersson, R. and B. Andersson: On the breakup of fluid particles in turbulent flows. *AIChE Journal* vol. 52 no. 6: (2006) 2020-2030.

[5] Vejražka, M. Zedníková, P. Stanovský: Characterisation of turbulent flow in a breakup cell. *Proceedings of the International Conference Experimental Fluid Mechanics 2016*, Mariánské Lázně, Czech Republic, 15-18 November 2016, pp. 890-896.

[6] Zedníková, M., Vejražka, J., Stanovský, P.: Experiments on bubble and drop breakup in a turbulent flow. *Proceedings of the International Conference Experimental Fluid Mechanics 2016*, Mariánské Lázně, Czech Republic, 15-18 November 2016, pp. 964-969.

[7] Xing, Ch., Wang, T., Guo, K., Wang, J.: A unified theoretical model for breakup of bubbles and droplets in turbulent flow. *AIChE Journal*, vol. 61 no. 4: (2015) pp. 1391-1403.

[8] Brenner, M. P., S. Hilgenfeldt and D. Lohse: Single-bubble sonoluminescence. *Reviews of Modern Physics* vol. 74 no. 2: (2002) pp. 425-484.

[9] Bolanos-Jimenez, R., A. Sevilla and C. Martinez-Bazan: The necking time of gas bubbles in liquids of arbitrary viscosity. *Physics of Fluids* vol. 28 no. 4: (2016) article no. 042105.

[10] Luo, H. and H. F. Svendsen: Theoretical model for drop and bubble breakup in turbulent dispersions. *AIChE Journal* vol. 42 no. 5: (1996) 1225-1233.